Investigating the Role of Sulfate Groups for the Binding of Gd³⁺ Ions to Glycosaminoglycans with NMR Relaxometry

Patrick Werner+,[a, b, c] Patrick Schuenke+,[b, d] Oxana Krylova,[b] Heike Nikolenko,[b] Matthias Taupitz,[c] and Leif Schröder*[a, b, c]

Glycosaminoglycans (GAGs) are highly negatively charged macromolecules with a large cation binding capacity, but their interaction potential with exogeneous Gd³⁺ ions is under-investigated. These might be released from chelates used as Gadolinium-based contrast agents (GBCAs) for clinical MR imaging due to transmetallation with endogenous cations like Zn^{2+}. Recent studies have quantified how an endogenous GAG sequesters released Gd³⁺ ions and impacts the thermodynamic and kinetic stability of some GBCAs. In this study, we investigate and compare the chelation ability of two important GAGs (heparin and chondroitin sulfate), as well as the homopolysaccharides dextran and dextran sulfate that are used as models for alternative macromolecular chelators. Our combined approach of MRI-based relaxometry and isothermal titration calorimetry shows that the chelation process of Gd³⁺ into GAGs is not just a long-range electrostatic interaction as proposed for the Manning model, but presumably a site-specific binding. Furthermore, our results highlight the crucial role of sulfate groups in this process and indicate that the potential of a specific GAG to engage in this mechanism increases with its degree of sulfation. The transchelation of Gd³⁺ ions from GBCAs to sulfated GAGs should thus be considered as one possible explanation for the observed long-term deposition of Gd³⁺ *in vivo* and related observations of long-term signal enhancements on T_1-weighted MR images.

Introduction

Low molecular weight Gadolinium-based contrast agents (GBCAs) are widely used in clinical magnetic resonance imaging (MRI) examinations. Chelated Gd³⁺ ions with one coordination site for water enhances the longitudinal relaxation rate (R_1) of water protons and thus yields positive (bright) image contrast from tissue with increased GBCA concentration. For a long time, these agents were assumed to be inert and excreted from the human body as intact compounds and therefore to be harmless for patients even after multiple administrations.[1–6] However, in the last decade several studies questioned the safety of GBCAs and associated the occurrence of nephrogenic systemic fibrosis (NSF) and Gadolinium (Gd) long-term depositions with prior administrations of GBCAs. As a consequence, the use of certain GBCAs has already been restricted by the European Medicines Agency (EMA) and the U.S. Food and Drug Administration (FDA).[7,8] Especially linear GBCAs were shown to have a reduced thermodynamic stability compared to macrocyclic ones and were thus classified to be prone to release their central Gd³⁺ ion due to the replacement with competing cations.[9–11] This process named transmetallation is well studied using various scientific approaches including NMR relaxometry.[9,12–17] However, it is now established that all GBCAs can lead to Gd³⁺ ion deposition in the human body, but the interaction of dissociated Gd³⁺ ions with endogenous substances in the human body is still under-investigated.[18,19] Understanding the related mechanisms is a persisting task at the interface between chemistry, biology, and contrast agent design to ensure optimum safety of future formulations.[18] To explain the observed long-term signal enhancements on MRI scans *in vivo*, several studies concluded that the dissociated Gd³⁺ ions must partially be re-chelated by macromolecular species that subsequently exhibit high T_1 relaxivity values due to a reduced rotational tumbling rate.[16,17,20,21] In addition to a large molecular size, the potential new chelator structure needs to provide a good accessibility for dissociated Gd³⁺ ions and, based on the diversity of reported deposition sites in the human body, be ubiquitous distributed throughout the entire body.

In previous studies, we showed that the glycosaminoglycan (GAG) heparin is a suitable candidate for such a macromolecular

[a] Dr. P. Werner,+ Dr. L. Schröder
    Division of Translational Molecular Imaging
    Deutsches Krebsforschungszentrum (DKFZ)
    Im Neuenheimer Feld 280, 69120 Heidelberg (Germany)
    E-mail: leif.schroeder@dkfz.de
[b] Dr. P. Werner,+ Dr. P. Schuenke,+ Dr. O. Krylova, H. Nikolenko, Dr. L. Schröder
    Molecular Imaging / Molecular Biophysics
    Leibniz-Forschungsinstitut für Molekulare Pharmakologie (FMP)
    Robert-Rössle-Str. 10, 13125 Berlin (Germany)
[c] Dr. P. Werner,+ Prof. Dr. M. Taupitz, Dr. L. Schröder
    Department of Radiology
    Charité – Universitätsmedizin Berlin, corporate member of Freie Universität Berlin,
    Humboldt-Universität zu Berlin, and Berlin Institute of Health
    Charitéplatz 1, 10117 Berlin (Germany)
[d] Dr. P. Schuenke+
    Department of Biomedical Magnetic Resonance
    Physikalisch-Technische Bundesanstalt (PTB), Braunschweig and Berlin
    Abbestraße 2–12, 10587 Berlin (Germany)
[+] These authors contributed equally to this work.

Supporting information for this article is available on the WWW under https://doi.org/10.1002/cmdc.202100764

ChemMedChem

Research Article
doi.org/10.1002/cmdc.202100764

Chemistry
Europe
European Chemical
Societies Publishing

chelator.[16,17] GAGs are macromolecular, negatively charged endogenous polysaccharides and represent an integral part of the human glycome. The structural diversity of GAGs and their distribution in the extracellular matrix (ECM), on cell surfaces, and in cells illuminate their physiological significance and make them important candidates for interactions with Gd^{3+} ions.[22,23] Within this group of polysaccharides, sulfation is an important feature mostly known for its modulation of extracellular signals such as cell-cell and cell-matrix interactions. The degree of GAG sulfation controls its negative charge and is the main driver for extracellular matrix interactions with proteins. GAGs also promote extracellular cation homeostasis.[24] Besides heparin, examples for endogenous GAGs are chondroitin sulfate, heparan sulfate, hyaluronic acid, dermatan sulfate, and keratan sulfate.[25–28]

While it is intuitively clear that GAGs could interact with cations due to their negatively charged carboxyl and sulfate groups, the mechanisms of interactions are indeed complex and depend on the type of the participating cation as well as on the GAG functional groups.[29] In general, two different binding mechanisms have been proposed: the first one, named territorial binding, is a long-range electrostatic interaction, where the ions remain unlocalized and exhibit an unrestricted mobility according to the Manning counter ion condensation model.[29,30] The second proposed type of binding is a site-specific chelation. While the territorial binding retains full hydration ($q = 8$ for Gd^{3+}) and almost unrestricted mobility of the ions, the site-specific binding has more strict geometrical requirements including a fixed number of coordinating groups resulting in lower hydration numbers. Both types of binding have been reported for the binding of cations within GAGs, i.e., territorial binding for Mg^{2+} and, with some controversy, for Ca^{2+}. Site-specific chelation has been described for Zn^{2+} and La^{3+}.[31] As both the different degree of hydration and ion mobility are parameters that critically influence the relaxivity of bound Gd^{3+} ions and thus the observable T_1 relaxation time of solvent water, quantitative NMR relaxometry should be suitable to distinguish between the two types of binding.[17]

Therefore, the goal of this study was to apply a combination of quantitative MRI-based relaxometry and isothermal titration calorimetry (ITC) to qualitatively investigate the type of binding between Gd^{3+} ions and polysaccharide model substances. The previously observed pronounced differences for the water proton relaxivity caused by Gd^{3+} ions in different molecular environments should also be capable of providing valuable insights into the chelation ability of carefully chosen GAG models and its dependence on their degree of sulfation (e.g., heparin and chondroitin sulfate A; Figure 1). The methods proposed here shall assist in contributing to the discussion regarding potential interactions between exogenous Gd^{3+} ions and endogenous substances.
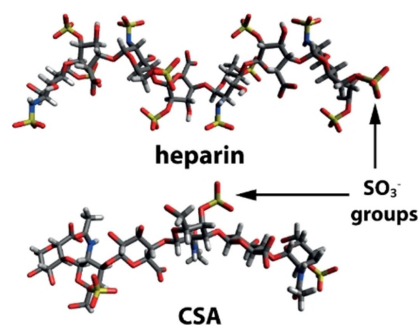

Figure 1. Fragment structures of investigated glycosaminoglycans heparin and chondroitin sulfate A (CSA). Illustrations are based on structures from the Protein Data Bank (PDB) for highlighting differences in the sulfation pattern of these polysaccharides.

Results and Discussion

Binding of gadolinium to GAGs

All ^{1}H NMR relaxometry investigations are based on the fact that the binding of Gd^{3+} ions to different chelator structures results in different relaxivities. In a first step, we thus determined the relaxivities of $GdCl_3$ in all substances investigated within this study. For quantifications, five different $GdCl_3$ concentrations and a fixed amount of the different chelator structures were used. Figure 2a shows the setup to enable the simultaneous measurement of multiple sample solutions under identical experimental conditions. The quantitative evaluation (see Materials and Methods) yields relaxation rate (R_1) maps as output (Figure 2b).

The determined relaxivity values obtained from R_1 maps with samples of different concentrations are listed in Table 1. The corresponding measured relaxation rates and linear fits are shown in Supporting Information Figures S2–S4.
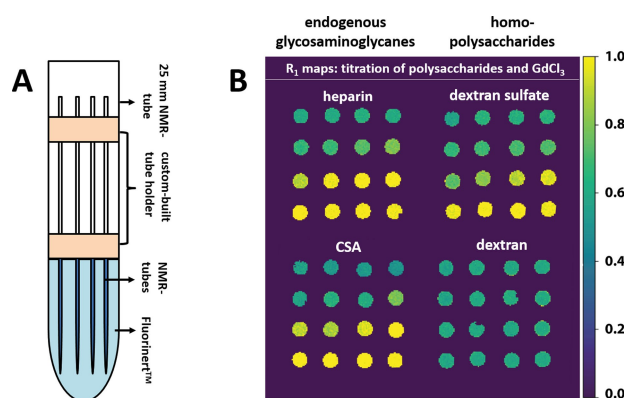
Figure 2. (A) Schematic overview of the exemplary experimental setup of an NMR relaxometry measurement in a 25 mm coil. (B) Representative R_1 maps of the titration experiments of $GdCl_3$ with the endogenous glycosaminoglycans heparin (top left) and CSA (bottom left) and with the homopolysaccharides dextran sulfate (top right) and dextran (bottom right). All quantitative values in the manuscript are given by the ROI-averaged mean±SD of ten such independently acquired maps.

ChemMedChem

Research Article
doi.org/10.1002/cmdc.202100764

**Chemistry
Europe**

European Chemical
Societies Publishing

Table 1. Water proton relaxivities for dissolved GdCl$_3$ in different environments.

Sample	r_1 [s^{-1} mM^{-1}]
GdCl$_3$ in heparin	26.51 ± 0.26
GdCl$_3$ in CSA	23.48 ± 1.44
GdCl$_3$ in dextran sulfate	20.38 ± 1.55
GdCl$_3$ in dextran	11.48 ± 0.03
GdCl$_3$ in water	11.43 ± 0.31

To investigate the chelation capacity of the different chelator structures for Gd^{3+} ions, we then performed titration experiments with a fixed concentration (4.6 mg/L) of GdCl$_3$ and varying concentrations of the investigated chelator structures. This results in an increasing transformation from low to high relaxivity compounds with the increasing availability of chelator structures. Consequently, the measured R_1 titration curves of heparin and CSA start at values of $R_1 \approx 0.63 \pm 0.01$ s^{-1} and $R_1 \approx 0.64 \pm 0.01$ s^{-1}, respectively (Figure 3). Both values match the expected relaxation rate of 4.6 mg/L (25 μM) GdCl$_3$ in nanopure water. With increasing concentration ratios, the measured R_1 values increase till both curves asymptotically approach new plateau values. In the plateau, it can be assumed that all Gd^{3+} ions are bound to the chelator structure. The two plateaus (new chemical equilibria) in Figure 3a are characterized by $R_1 \approx 1.03 \pm 0.01$ s^{-1} for heparin and $R_1 \approx 0.96 \pm 0.01$ s^{-1} for CSA, respectively. These match the expected relaxation rates for 4.6 mg/L GdCl$_3$ in heparin ($R_1 \approx 1.01$ s^{-1}) and CSA ($R_1 \approx 0.94$ s^{-1}) solution, which can be calculated using the independently determined relaxivities from Table 1. The inflection points of the fitted logistic functions are reached at mass ratios of $x_0 = 1.16 \pm 0.06$ for heparin and $x_0 = 3.94 \pm 0.22$ for CSA. This means that the curve for CSA, which has less sulfate groups per disaccharide unit (range: 0.1-1.3, mean 0.7) compared to heparin (~ 2.7 sulfate groups per disaccharide unit), is shifted towards higher concentrations.[24,32] The shift in
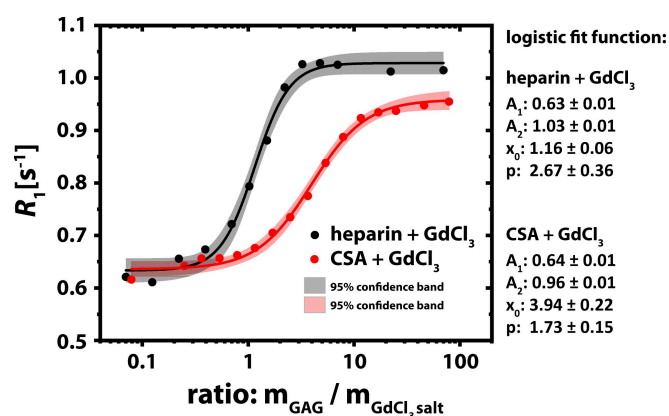
x_0 relates to about ~ 3.4 times more chelator material needed to bind the same amount of Gd^{3+} ions, which is consistent with the theoretical sulfate group per disaccharide unit ratio of $2.7/0.7 \approx 3.9$. The plotted 95% confidence bands show the good data quality of both data sets.

Binding of gadolinium to dextran sulfate and dextran

Figure 4 shows the titration curves for dextran and dextran sulfate that we used as well-defined models for sulfated and non-sulfated macromolecular chelators. As before, both titration curves start at R_1 values that match the expected relaxivity ($R_1 \approx 0.64$ s^{-1}) of 4.6 mg/L (25 μM) of GdCl$_3$ in nanopure water. For dextran sulfate, the R_1 values increase with increasing concentration ratios and asymptotically approach a new chemical equilibrium characterized by $R_1 \approx 0.85 \pm 0.01$ s^{-1}. This value is about 17% lower compared with the plateau value of heparin. The inflection point of the fitted logistic function for dextran sulfate is reached at a mass ratio of $x_0 = 2.03 \pm 0.18$. This value is in between the determined values for heparin ($x_0 = 1.16 \pm 0.06$) and CSA ($x_0 = 3.94 \pm 0.22$). The steepness of the transition is described by the fit parameter p. Again, the determined value for dextran sulfate ($p = 2.03 \pm 0.18$) is between the determined values for heparin ($p = 2.67 \pm 0.36$) and CSA ($p = 1.73 \pm 0.15$). Most important, no significant changes of R_1 could be observed for the titration of GdCl$_3$ in non-sulfated dextran solution (green circles). This indicates that the absence of sulfate groups comes along with the loss of the chelation ability for Gd^{3+} ions.

Isothermal titration calorimetry

To confirm our hypothesis drawn from Figure 4, we used the well-established ITC technique to determine the thermodynam-
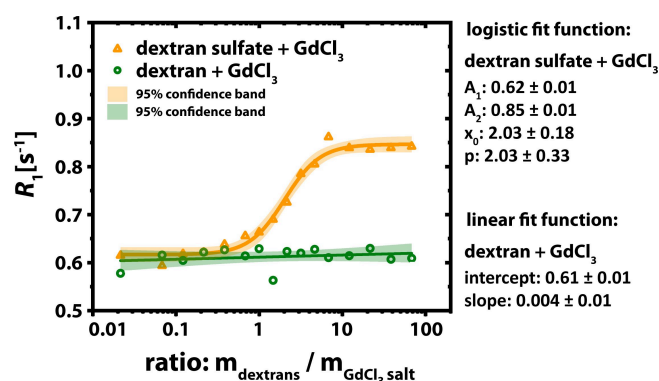

logistic fit function:

heparin + GdCl$_3$
A$_1$: 0.63 ± 0.01
A$_2$: 1.03 ± 0.01
x_0: 1.16 ± 0.06
p: 2.67 ± 0.36

CSA + GdCl$_3$
A$_1$: 0.64 ± 0.01
A$_2$: 0.96 ± 0.01
x_0: 3.94 ± 0.22
p: 1.73 ± 0.15

Figure 3. R_1 titration curves with corresponding 95% confidence band of GdCl$_3$ with the glycosaminoglycans heparin (black) and CSA (red). Each data point represents ROI-averaged mean values of ten independently acquired R_1 maps. Both curves initially match the expected relaxivity of 4.6 mg/L (25 μM) of GdCl$_3$ in nanopure water. The inflection points are reached at a mass ratio of about 1.16 and 3.94 for heparin and CSA, respectively.

logistic fit function:

dextran sulfate + GdCl$_3$
A$_1$: 0.62 ± 0.01
A$_2$: 0.85 ± 0.01
x_0: 2.03 ± 0.18
p: 2.03 ± 0.33

linear fit function:

dextran + GdCl$_3$
intercept: 0.61 ± 0.01
slope: 0.004 ± 0.01

Figure 4. R_1 titration curves with corresponding 95% confidence band of GdCl$_3$ with the homopolysaccharides dextran sulfate (orange triangles) and dextran (green circles). Each data point represents ROI-averaged mean values of ten independently acquired R_1 maps. Both curves initially match the expected relaxivity of 4.6 mg/L (25 μM) of GdCl$_3$ in nanopure water. Only the curve of dextran sulfate increases with increasing mass ratios until a new plateau value of $R_1 \approx 0.85$ s^{-1} is reached. The inflection point is reached at a mass ratio of 2.03.

ChemMedChem

Research Article
doi.org/10.1002/cmdc.202100764

**Chemistry
Europe**

European Chemical
Societies Publishing

ic parameters of the mentioned chelation processes. Figure 5 shows the investigation of the binding effect between Gd^{3+} ions and dextran (green) as well as between Gd^{3+} ions and dextran sulfate (orange) by ITC measurements. In subfigure 5 A, the endothermic raw data of the titration results is shown and subfigure 5B displays the integrated amounts of heat of injection against molar ratio of reactants and corresponded binding curve with the best data fit. A strong interaction between dextran sulfate and Gd^{3+} ions could be observed. This is characterized by $\Delta G^0 = -8.53$ kcal/mol and a rather high binding affinity with $K_D = 559 \pm 144$ nM. A thermodynamically unfavorable endothermic enthalpy change, $\Delta H^0 = 3.35 \pm 0.04$ kcal/mol of Gd^{3+} ions binding to dextran sulfate was compensated with the strong entropic contribution, $-T\Delta S^0 = -11.9$ kcal/mol. The stoichiometry of the binding complex, $n = (4.50 \pm 0.03)$, indicates multiple Gd^{3+}-binding sites on long dextran sulfate molecules. In agreement with the results from Figure 4, no binding could be observed for the non-sulfated dextran (green circles).

Taken together, MRI-based relaxometry and ITC and revealed that sulfate groups play a crucial role for the overall transchelation process. Further analysis will also show that the binding is presumably site-specific and not simply a long-range electrostatic interaction.

Under physiological conditions, Gd^{3+} ions do not occur in the human body. However, in recent years many studies reported the detection of this toxic heavy metal ion in various tissues in the human body.[10,11,20,33,34] The dissociation of Gd^{3+} ions from their parent GBCA complexes during clinical examinations were mentioned as a major reason for these occurrences. The deposition of Gd^{3+} ions in various tissues after repeated applications of GBCAs was first observed as hyperintensities on unenhanced T_1-weighted MRI images up to several month after the last GBCA administration and afterwards confirmed by post-mortem tissue analyzes. Nevertheless, the health consequences

of these Gd^{3+} ion deposition are still largely unknown and further studies on possible long-term effects are necessary.[35] To investigate the tissue deposition of Gd^{3+} ions in more detail, it is of great importance to know more about the different endogenous species that can interact with the dissociated ions.

In general, many different structures are conceivable as binding partners for dissociated Gd^{3+} ions. However, based on the diversity of reported Gd^{3+} ion deposition sites, it can be concluded that these species must be ubiquitously distributed throughout the human body and be easily accessible for dissociated Gd^{3+} ions. Potential candidates that fulfil these prerequisites are endogenous structures like transferrin, albumin, and citrate. Furthermore, due to their ubiquitous presence in the human body, and their large molecular size of several kDa, GAGs represent another promising group of substances. As their potential to serve as binding partners for dissociated Gd^{3+} ions was shown before, we also focused on the investigation of GAGs in this study.[16,17]

The GAGs used in our experiments represent only a small selection from the large family of polysaccharides, but they were chosen with mindful consideration: chondroitin sulfate is the most abundant GAG in the central nervous system and represents the main sugar component in GAG-rich perineuronal networks in different part of the brain (entorhinal cortex, amygdala, hippocampus, motor and somatosensory cortex, visual cortex, and prefrontal cortex).[36] Heparin, on the other hand, is the most negatively charged GAG in the human body with an average of 2.7 sulfate groups per disaccharide unit.[32] In the human organism, it can be found in the context of inflammatory reactions. The potential of heparin to bind Gd^{3+} ions has recently been proven employing NMR relaxometry.[16,17] However, this had never been shown for CSA or any other GAG before.

To investigate the interaction of Gd^{3+} ions with the selected GAG structures, we performed titration experiments revealing
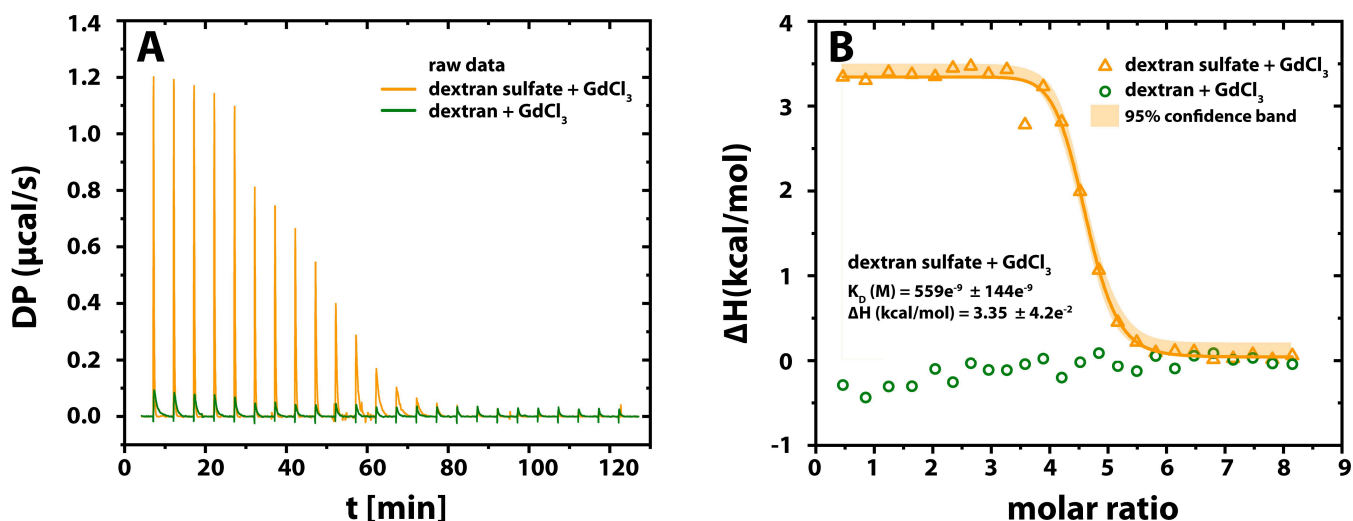

Figure 5. Results of ITC measurements to analyze the binding of Gd^{3+} to dextran sulfate and dextran in Na-acetate buffer (pH = 6.0). Both polysaccharides were titrated over 24 injections in aqueous $GdCl_3$ solution ([Gd^{3+}] = 2 mM). (A) raw titration data of the endothermic reaction for dextran sulfate (orange) and dextran (green). (B) corresponding integrated data and the fit result (solid orange line) including the 95% confidence band for dextran sulfate. The interaction between dextran sulfate and Gd^{3+} ions is expressed by a K_D of 559 ± 144 nM, while no interaction/binding could be observed between dextran and Gd^{3+}.

ChemMedChem

Research Article
doi.org/10.1002/cmdc.202100764

**Chemistry
Europe**
European Chemical
Societies Publishing

pronounced differences in relaxation behavior (Figure 3). From these experiments, we first conclude that a binding of Gd^{3+} ions into GAG structures takes place and secondly, that this is presumably a site-specific chelation where the capacity strongly depends on the degree of sulfation of the GAG. The first conclusion can be drawn from the significantly enhanced relaxation rates for increasing polysaccharide concentrations. Because the amount of paramagnetic Gd^{3+} ions stays constant for all sample solutions, the increasing relaxation rates must originate from increasing relaxivities. The observed relaxation rates for the new chemical equilibria are in good agreement with the high relaxivity values for polysaccharide-bound Gd^{3+} ions that we determined in independent experiments (Table 1). These high relaxivity values are most likely caused by the high molecular weight of the resulting macromolecular Gd^{3+}-GAG complexes, which leads to a reduced rotational tumbling rate and thus to more effective ^1H NMR relaxation.[17]

A side effect of increasing polysaccharide concentrations might be an increased viscosity that could also impact the observed relaxivity. But the observation that stable plateaus are reached in Figure 3 together with our previous calibration measurements indicate that this effect can be neglected for the GAG concentrations used in this study.[17]

This recent relaxometry calibration also supports the hypothesis that the magnitude of the transitions in Figure 3 is indicative for a site-specific binding of Gd^{3+} rather than an unlocalized interaction. Only site-specific binding with limited ion mobility (and limited hydration) should yield the observed highly increased relaxivity values. The alternative territorial binding of metal ions according to the Manning model should yield a relaxivity more similar to that of free aqueous Gd^{3+} due to full ion hydration (as assessed from $GdCl_3$ solutions) and unrestricted freedom of motion within a cylindrical condensation volume around the GAG.[30,31]

The concept of a specific binding is also supported by previously reported changes in ^1H NMR chemical shifts of heparin upon addition of La^{3+} ions, which have a similar ion radius compared to Gd^{3+} ions. These shifts have been interpreted as a combination of through-bond inductive effects and changes in conformation induced by a site-specific binding.[31] Importantly, the same study reports the binding constant for the La^{3+}-heparin complex to be larger than for the

divalent metal ions. This observation was ascribed to both a larger entropic contribution and a larger site-specific contribution. Also, the CO_2^- form of heparin has been reported to undergo a conformational change of the IdoA(2S)-ring upon addition of La^{3+} ions (an increased population of the $^1C_4$ conformation).[31] We thus conclude that Gd^{3+} ions are involved in similar site-specific interactions and that these are the origin for the observed large relaxivity changes.

In comparison to CSA, heparin is both more negatively charged and provides more sulfate groups per disaccharide unit.[24] Its most common disaccharide, IdoA(2S)-GlcNS(6S), has three sulfate groups, while CSA is only sulfonated at carbon 4 of the N-acetylgalactosamine (GalNAc). Both the higher degree of sulfation and also the other structural differences (in CSA, the GalNAc unit alternates only with glucuronic acid) can explain the earlier transition in the titration curves for heparin compared to CSA (Figure 3). For meaningful interpretation of this titration data, we employed the mass ratios of the polysaccharides to $GdCl_3$ instead of the concentration ratios. This overcomes the misleading influence of the different molecular masses of heparin and CSA and enables statements closely linked to the degree of sulfation of both GAGs. Due to the similar relaxivities (c.f. Table 1), we conclude that the binding type is presumably site-specific for both GAGs. In case of heparin, the polymeric chain could somewhat wrap around the Gd^{3+} ions. A qualitative model that is not based on structural data but an adaptation of the heparin structure (PDB entry: 3IRI) is given in Figure 6 to illustrate that multiple sulfate groups are in suitable proximity to the Gd^{3+} ions and possibly serve as ligands

However, it should be mentioned that the sheer presence of sulfate groups is not a warrant for their participation in (site-)specific metal ion binding. Whitfield et al. have shown that heavy metals bind only to certain heparin disaccharides. They investigated the interaction of Zn^{2+} ions with disaccharides made of IdoA2S with AnManOH(6S) or GlcNS(6S)αMe and observed a chelation only in the case of IdoA2S(α1,4)GlcNS(6S)αMe.[37] Site-specific binding can cause conformational changes as reported for the case of Zn^{2+} ions, which controls the ring conformation of iduronate in heparin and heparan sulfate.[37] Such "induced fit" might stabilize cation binding if it occurred also for Gd^{3+} ions and could contribute to
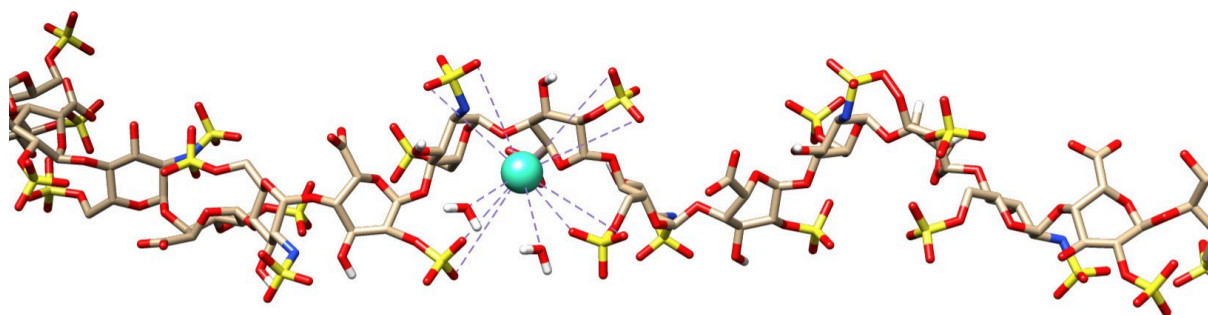

Figure 6. Schematic model of a chelated Gd^{3+} ion to heparin based on adaptation of the PDB structure 3IRI of heparin in solution. Multiple sulfate groups could wrap around the cation and serve as ligands for Gd^{3+}.

ChemMedChem

Research Article
doi.org/10.1002/cmdc.202100764

Chemistry
Europe
European Chemical
Societies Publishing

the observed high relaxivity. NMR studies also identified a general participation of the carboxylate and ring oxygen of IdoA2S residues in Zn^{2+} ions binding. This role of the oxygens in IdoA2S is consistent with the known coordination potentials of anionic groups such as carboxyl groups.[38] To further examine our hypothesis about the importance of the degree of sulfation of the investigated GAGs and to minimize the impact of other structural aspects, we used the homopolysaccharides dextran and dextran sulfate. The advantage of using these homopolysaccharides is their identical molecular mass of the backbone and matching length as well as the clear differentiation between a sulfated and a sulfate-free structure. The result from the MRI-based relaxometry experiments (Figure 4) demonstrated that dextran, in contrast to dextran sulfate, does not cause any significant change of the measured relaxation rate. This supports the assumed importance of the sulfate groups. However, the considerable problem of all conclusions drawn from the presented NMR-based experiments is that they only show the indirect effects of the chelation of Gd^{3+} ions to the polysaccharide structures, but not the chelation/binding process itself.

It should be mentioned that the relaxometric titration curves have been used in this study only for qualitative assessment regarding a ranking of the chelation potential for different polysaccharides based on relative shift of the point of inflection (CSA vs. heparin) or the lack of any step function (dextran vs. dextran sulfate). One might initially consider to apply fitting methods known from characterizing protein-ligand affinities where the definition of K_d yields a quadratic equation that can be solved to obtain a fitting function. When plotting the data against a linear abscissa, the quality of the result for K_d is very sensitive to the data points in the curvature that describes the transition from the initial steep linear increase to the final part of the square root function. Unfortunately, the relaxometric approach requires a certain amount of Gd^{3+} ions to obtain observable signal changes. In combination with the step-wise addition of the polysaccharides, we realized that under these conditions the kink in the transition towards high GAG concentrations is too sharp to obtain a reliable K_d value. To support our conclusions drawn from the NMR experiments, we therefore used ITC measurements. ITC is an established analytical method that is specifically tailored to this type of question. It quantifies chemical interactions in solution and is sensitive to enthalpy changes due to the chemical binding affinity of different molecules. Using ITC, we could confirm the crucial role of sulfate groups for the binding process: we could proof a binding between Gd^{3+} ions and dextran sulfate but not between Gd^{3+} ions and the non-sulfated dextran. Furthermore, the ITC measurements allowed to quantify the binding between the different substances. The very efficient binding between dextran sulfate and Gd^{3+} ions was expressed by a K_D of 559 ± 144 nM, which equals a log K_D of −6.25. This affinity is less efficient in comparison to the high desired stability of clinically used GBCAs with log K_D values around 20, but still reflects a significant affinity if no strong competition occurs inside the GAG matrix.[39,40]

Conclusion

Summarized, we could show that the binding of Gd^{3+} ions into GAG structures is presumably a site-specific binding that is characterized by a restricted ion mobility and limited hydration and therefore leads to very high relaxivity values of the resulting Gd^{3+}-GAG complexes. Furthermore, the combined results of our MRI and ITC measurements of dextran and dextran sulfate, as well as the results of our CSA and heparin measurements can serve as clear evidence that the degree of sulfation has a significant influence on this type of binding. On the one hand, this indicates that various sulfated GAGs besides heparin and CSA should have a chelation potential for Gd^{3+} ions. On the other hand, it also indicates that the absence of sulfate groups is presumably directly connected to the loss or at least a strong reduction of this chelation ability. This information might help to identify structures in the human body that are more likely to bind the Gd^{3+} ions that might dissociate from their parent GBCA structures due to transmetallation. It should consequently be considered to explain the mechanism behind the observed long-term retention of Gd^{3+} ions in the human body, particularly with regard to clinically observed hyperintense areas in MRI scans after multiple GBCA injections.

Experimental Section

$GdCl_3$ (Gadolinium (III) chloride hexahydrate, 99% titration) purchased from Sigma-Aldrich Chemie GmbH (Steinheim, Germany) served as a source for Gd^{3+} solutions. As model systems for human GAGs, a commercially available heparin solution (Heparin-Natrium-250000-ratiopharm®, 250000 IU/mL, average MW = 13 kDa, Ratiopharm GmbH (Ulm, Germany)) and chondroitin sulfate A (CSA, average MW = 20 kDa, Chondroitin 4-sulfate sodium salt from bovine trachea, Sigma-Aldrich Chemie GmbH, Steinheim, Germany) were used. Dextran and dextran sulfate (both as sodium salts from Leuconostoc spp. (MW ~ 40 kDa) and purchased from Sigma-Aldrich Chemie GmbH) were used in addition to the endogenous sugar structures to perform further NMR and ITC experiments. Millipore water (18 MΩ cm) was used for preparing all solutions. The chemicals required for this study were utilized as received without any further purification.

Quantitative MRI (qMRI) experiments were performed on a 9.4 T micro-imaging system (Bruker Biospin, Ettlingen, Germany) equipped with a 25 mm double-resonant ^{1}H/^{129}Xe transmit/receive coil (^{129}Xe channel not used). The ^{1}H T_1 relaxation time was determined using a dephasing recovery pulse sequence consisting of 50 non-selective π/2 pulses with interleaved gradient spoiling, followed by a varying recovery delay and a subsequent image readout. Spatial encoding was achieved with a gradient echo (GRE)-based, centric-reordered image readout, and the following parameters: $FoV = 20 \times 20$ mm², matrix size = 128×128, slice thickness = 2 mm, $BW = 50$ kHz, $TE = 2.5$ ms, $TR = 5.7$ ms. A variable temperature unit (VTU) served to control the sample temperature. Samples could stabilize for about 1 h after being put into the magnet to ensure a stable temperature of 25°C prior to data acquisition. All measurements were performed using custom-built tube holders that fit either seven (diameter $d = 5$ mm) or 16 ($d = 2.5$ mm) NMR tubes. The sample holders were immersed into a 25 mm glass tube filled with Fluorinert™ for improved susceptibility conditions between the individual samples. Quantitative R_1 ($= 1/T_1$) values were

ChemMedChem

Research Article
doi.org/10.1002/cmdc.202100764

Chemistry Europe
European Chemical
Societies Publishing

determined by fitting a mono-exponential function to the region of interest (ROI)-averaged data obtained for a set of different T_1-weighted images resulting from varying recovery times between 10 ms and 6 s. All shown values represent the average (± 1 SD) of 10 independent repetitions. The quantitative evaluation was performed using a python script that automatically masks the pixels outside the sample solutions and performs the data fitting with R_1 maps as final output.

NMR titration experiments were performed to investigate the binding of Gd^{3+} ions to heparin, CSA, dextran, and dextran sulfate using one set of 16 sample solutions, each. The sample solutions consisted of different polysaccharide concentrations between 0.033–3250 mg/L for heparin, between 0.366–366 mg/L for CSA, and between 0.1–316.2 mg/L for both dextran and dextran sulfate. Each solution further contained 4.6 mg/L (25 μM) of $GdCl_3$. The pH was not further adjusted in the relaxometry measurements to ensure better comparability with initial findings by Taupitz et al. and our recent work.[16,17] Overall, no further ions were added for the sake of minimizing the number of potential interaction partners. It should be noted that coordination equilibria are pH dependent. Therefore, the pH for all our samples was measured before and after the relaxometry experiments to ensure that experiments occur within a range where the ligands do not have protonation functions. This condition was fulfilled as the observed values always remained within in the range between 5.7 and 6.5 (see Supporting Information Figure S1). The influence of Gd-hydroxo complexes on the studied system should be considered negligible in this regime.

ITC was used to investigate the binding of Gd^{3+} ions to the clearly defined model substances dextran and dextran sulfate. Experiments were performed on MicroCal PEAQ-ITC microcalorimeter (Malvern Panalytical GmbH, Germany). Experiments were performed in 100 mM Na-acetate buffer, pH 6.0 at 25 °C. Despite the use of acetate groups as ligands in multidentate macrocyclic chelators, the formation of $Gd(OAc)_3$ complexes must be considered as a rather dynamic process in solution with different acetate complexes coexisting with free acetate groups. The lack of a backbone with its arranged multidentate constraints makes the as-formed Gd-acetate complexes rather labile. In comparison with the chelation of Gd^{3+} to the GAG structures with its arranged ligands, we therefore consider the stability of $Gd(OAc)_3$ complexes to be outperformed rather easily by the GAGs. The use of NaOAc buffer should be a minor perturbation of the chelation under investigation.

For dextran and dextran sulfate, 2 mM $GdCl_3$ was titrated in 2 to 3 μL steps into 50 μM polysaccharide solution in the calorimeter cell. The reaction mixture was continuously stirred at 750 rpm. Other experimental settings included a spacing time of 5 s and a filtering period of 5 s. For both experiments, the instrument software (MicroCal PEAQ-ITC Analysis) was used for baseline adjustment, peak integration, and normalization of the reaction heat with respect to the molar amount of injected ligand, as well as for data fitting and binding parameter evaluation. The binding experiments were corrected for the heat of $GdCl_3$ dilution, which had been determined separately ($GdCl_3$ titration into buffer). The potential residual formation of $Gd(OAc)_3$ (low stability) should not influence the ITC measurements in a significant way. Thus, it can be assumed that all recorded thermodynamic changes are due to the interaction of Gd^{3+} ions with dextran sulfate.

Acknowledgements

Conflict of Interest

The authors declare no conflict of interest.

Data Availability Statement

The data that support the findings of this study are available from the corresponding author upon reasonable request.

[1] J. Lohrke, T. Frenzel, J. Endrikat, F. C. Alves, T. M. Grist, M. Law, J. M. Lee, T. Leiner, K.-C. Li, K. Nikolaou, M. R. Prince, H. H. Schild, J. C. Weinreb, K. Yoshikawa, H. Pietsch, *Adv. Ther.* **2016**, *33*, 1–28.

[2] M. A. Kirchin, G. Pirovano, C. Venetianer, A. Spinazzi, *J. Magn. Reson. Imaging* **2001**, *14*, 281–94.

[3] V. Aslanian, H. Lemaignen, P. Bunouf, M. G. Svaland, A. Borseth, B. Lundby, *Neuroradiology* **1996**, *38*, 537–41.

[4] M. V. Knopp, T. Balzer, M. Esser, F. K. Kashanian, P. Paul, H. P. Niendorf, *Invest. Radiol.* **2006**, *41*, 491–9.

[5] C. U. Herborn, E. Honold, M. Wolf, J. Kemper, S. Kinner, G. Adam, J. Barkhausen, *Invest. Radiol.* **2007**, *42*, 58–62.

[6] V. M. Runge, J. R. Parker, *Eur. Radiol.* **1997**, *7 (Suppl. 5)*, 243–5.

[7] I. A. Dekkers, R. Roos, A. J. van der Molen, *Eur. Radiol.* **2018**, *28*, 1579–1584.

[8] L. Yang, I. Krefting, A. Gorovets, L. Marzella, J. Kaiser, R. Boucher, D. Rieves, *Radiology* **2012**, *265*, 248–253.

[9] S. Laurent, L. Vander Elst, F. Copoix, R. N. Muller, *Invest. Radiol.* **2001**, *36*, 115–22.

[10] A. Radbruch, L. D. Weberling, P. J. Kieslich, O. Eidel, S. Burth, P. Kickingereder, S. Heiland, W. Wick, H.-P. Schlemmer, M. Bendszus, *Radiology* **2015**, *275*, 783–91.

[11] T. Kanda, K. Ishii, H. Kawaguchi, K. Kitajima, D. Takenaka, *Radiology* **2014**, *270*, 834–41.

[12] L. Telgmann, C. A. Wehe, J. Künnemeyer, A. C. Bülter, M. Sperling, U. Karst, *Anal. Bioanal. Chem.* **2012**, *404*, 2133–2141.

[13] J. Künnemeyer, L. Terborg, S. Nowak, L. Telgmann, F. Tokmak, B. K. Krämer, A. Günsel, G. A. Wiesmüller, J. Waldeck, C. Bremer, U. Karst, *Anal. Chem.* **2009**, *81*, 3600–3607.

[14] M. Rasschaert, A. Emerit, N. Fretellier, C. Factor, P. Robert, J.-M. Idée, C. Corot, *Invest. Radiol.* **2018**, *53*, 328–337.

[15] S. Laurent, L. Vander Elst, C. Henoumont, R. N. Muller, *Contrast Media Mol. Imaging* **2010**, *5*, 305–308.

[16] M. Taupitz, N. Stolzenburg, M. Ebert, J. Schnorr, R. Hauptmann, H. Kratz, B. Hamm, S. Wagner, *Contrast Media Mol. Imaging* **2013**, *8*, 108–16.

[17] P. Werner, M. Taupitz, L. Schröder, P. Schuenke, *Sci. Rep.* **2021**, *11*, 21731.

[18] M. Le Fur, P. Caravan, *Metallomics* **2019**, *11*, 240–254.

[19] S. Bussi, A. Coppo, C. Botteron, V. Fraimbault, A. Fanizzi, E. De Laurentiis, S. Colombo Serra, M. A. Kirchin, F. Tedoldi, F. Maisano, *J. Magn. Reson. Imaging* **2018**, *47*, 746–752.

[20] E. Gianolio, E. Di Gregorio, S. Aime, *Eur. J. Inorg. Chem.* **2019**, *2019*, 137–151.

[21] P. Robert, S. Fingerhut, C. Factor, V. Vives, J. Letien, M. Sperling, M. Rasschaert, R. Santus, S. Ballet, J.-M. Idée, C. Corot, U. Karst, *Radiology* **2018**, *288*, 424–433.

[22] A. D. Lander, S. B. Selleck, *J. Cell Biol.* **2000**, *148*, 227–232.

[23] R. S. Aquino, E. S. Lee, P. W. Park, in *Progress in Molecular Biology and Translational Science.* Vol. 93. Elsevier Inc. **2010**. pp. 373–394.

[24] D. Soares da Costa, R. L. Reis, I. Pashkuleva, *Annu. Rev. Biomed. Eng.* **2017**, *19*, 1–26.

[25] K. Sugahara, T. Mikami, T. Uyama, S. Mizuguchi, K. Nomura, H. Kitagawa, *Curr. Opin. Struct. Biol.* **2003**, *13*, 612–620.

[26] B. Mulloy, J. Hogwood, E. Gray, R. Lever, C. P. Page, *Pharmacol. Rev.* **2015**, *68*, 76–141.

[27] A. Almond, *Cell. Mol. Life Sci.* **2007**, *64*, 1591–1596.

[28] S. Yamada, K. Sugahara, S. Özbek, *Commun. Integr. Biol.* **2011**, *4*, 150–158.

[29] M. Hricovíni, P. M. Nieto, G. Torri, in *NMR Spectroscopy of Glycoconjugates*. Vol. 2. Wiley-VCH Verlag GmbH & Co. KGaA, Weinheim, Germany **2002** pp. 189–229.

[30] G. S. Manning, *Acc. Chem. Res.* **1979**, *12*, 443–449.

[31] D. L. Rabenstein, J. M. Robert, J. Peng, *Carbohydr. Res.* **1995**, *278*, 239–56.

[32] I. Capila, R. J. Linhardt, *Angew. Chem. Int. Ed. Engl.* **2002**, *41*, 391–412.

[33] G. W. White, W. A. Gibby, M. F. Tweedle, *Invest. Radiol.* **2006**, *41*, 272–278.

[34] S. Sanyal, P. Marckmann, S. Scherer, J. L. Abraham, *Nephrol. Dial. Transplant.* **2011**, *26*, 3616–3626.

[35] J. Ramalho, R. C. Semelka, M. Ramalho, R. H. Nunes, M AlObaidy, M. Castillo, *Am. J. Neuroradiol.* **2016**, *37*, 1192–1198.

[36] K. Sugahara, T. Mikami, *Curr. Opin. Struct. Biol.* **2007**, *17*, 536–545.

[37] D. M. Whitfield, J. Choay, B. Sarkar, *Biopolymers* **1992**, *32*, 585–596.

[38] G. Pass, G. O. Phillips, D. J. Wedlock, R. G. Morley, in *Carbohydrate Sulfates*, American Chemical Society, **1978**, pp. 259–281.

[39] A. D. Sherry, W. P. Cacheris, K. T. Kuan, *Magn. Reson. Med.* **1988**, *8*, 180–190.

[40] T. Frenzel, P. Lengsfeld, H. Schirmer, J. Hütter, H.-J. Weinmann, *Invest. Radiol.* **2008**, *43*, 817–828.